Optimised Reproduction of Coupled Longitudinal-Lateral Pre-Crash Accelerations Using a Rotated Low-G Sled Setup

Niklas Fahse, Philipp Rodegast, Felix Ressi, Desiree Kofler, Corina Klug, Jörg Fehr

I. INTRODUCTION

Holistic vehicle safety [1] requires consideration of the pre-crash phase, in particular accidents on curved rural roads and highway entry or exit ramps can generate coupled longitudinal–lateral vehicle accelerations that can lead to significant variability in occupant posture and kinematics prior to impact [2]. This variability creates challenges for the modelling and validation of low-acceleration events. Digital Human Models (DHMs) provide a powerful tool to assess occupant comfort, safety, and biomechanical response under a wide range of loading directions and boundary conditions. Using such models enables the prediction of occupant interactions with the integrated safety systems, including seat belt pretensioners and autonomous emergency braking (AEB), during the pre-crash phase - occupant motion until impact t_{Zero}. However, simulation results require experimental validation. This study investigates how well an optimised longitudinal–lateral acceleration pulse, realisable on a rotated low-G sled test environment, can reproduce real coupled pre-crash kinematics and how the choice of optimisation metric influences the resulting kinematic responses.

II. METHODS

Pre-crash vehicle trajectories were reconstructed using PC-Crash based on accident cases from the CEDATU and GIDAS databases. Vehicle accelerations were expressed in the vehicle coordinate system as longitudinal $\boldsymbol{a_x(t_i)}$, and lateral $\boldsymbol{a_y(t_i)}$, components, sampled at equidistant time steps $\Delta t = 10\ ms$ from t_{start} to t_{Zero} (time of crash). From the CEDATU reconstructions, multi-axis acceleration pulses were clustered using k-means clustering to identify representative pre-crash motion patterns. One cluster characterised by strongly coupled longitudinal and lateral accelerations was selected as representative. Acceleration pulses reconstructed from GIDAS UTYP 141 [three (Run-off-road accident)] were subsequently compared with the centroid of this representative cluster. Similarity was quantified using the Euclidean distance between normalised acceleration time histories. Two distinct matches were identified as Pulse 33 (RMSE = 0.98 m s^{-2}) and Pulse 40 (RMSE = 1.104 m s^{-2}) (Fig. 1a, coloured lines) of the data provided by TU Dresden within the TC i-protect consortium and the SAFE-X project partners.

Several experimental approaches can be used to investigate occupant behaviour during pre-crash manoeuvres. Full-vehicle tests provide high realism but require complex instrumentation and offer limited repeatability. Traditional sled tests represent the standard laboratory approach, but they typically reproduce one-dimensional acceleration pulses and often lack visual feedback for human subjects. The Low-G sled testbench at TU Graz [5] enables controlled reproduction of low-acceleration pulses representative of pre-crash manoeuvres. In this setup, the seat can be rotated along the vertical axis, allowing the emulation of combined longitudinal–lateral loading conditions.

To approximate the reconstructed two-dimensional vehicle pulse, the seat orientation was determined by an orthogonal least-squares projection of the longitudinal–lateral acceleration vector onto the principal eigenvector of $\boldsymbol{S} = \begin{bmatrix} \sum \boldsymbol{a}_x^2(\boldsymbol{t_i}) & \sum \boldsymbol{a}_x(\boldsymbol{t_i})\boldsymbol{a}_y(\boldsymbol{t_i}) \\ \sum \boldsymbol{a}_y(\boldsymbol{t_i})\boldsymbol{a}_x(\boldsymbol{t_i}) & \sum \boldsymbol{a}_y^2(\boldsymbol{t_i}) \end{bmatrix}$. The angle of the optimal direction is $\theta = \frac{1}{2}\operatorname{atan}\left(2\sum \boldsymbol{a}_x(\boldsymbol{t_i})\boldsymbol{a}_y(\boldsymbol{t_i}), \sum \boldsymbol{a}_x^2(\boldsymbol{t_i}) - \sum \boldsymbol{a}_y^2(\boldsymbol{t_i})\right)$. The projected pulse $\boldsymbol{p(t)} = \boldsymbol{a}_x(t)\cos\theta + \boldsymbol{a}_y(t)\sin\boldsymbol{\theta}$ minimises the deviation between the reproduced acceleration $\widehat{\boldsymbol{a}} = \begin{bmatrix} \widehat{\boldsymbol{a}}_x \\ \widehat{\boldsymbol{a}}_y \end{bmatrix} = \begin{bmatrix} \boldsymbol{p(t)}\cos\theta \\ \boldsymbol{p(t)}\sin\theta \end{bmatrix}$ and the original acceleration signal $\boldsymbol{a} = \begin{bmatrix} \boldsymbol{a}_x \\ \boldsymbol{a}_y \end{bmatrix}$. The projected acceleration signal was numerically integrated to obtain the corresponding sled velocity and displacement over time. Due to the limited sled displacement, the projected signal is cropped to show only the final segment of the pulse.

N. Fahse and P. Rodegast are Research Associates and Doctoral Students, J. Fehr (+49 711 685 66392; joerg.fehr@itm.uni-stuttgart.de) is a Professor at Institute of Engineering and Computational Mechanics, University of Stuttgart, Germany. F. Ressi is a Senior Project Scientist, D. Kofler is a researcher and C. Klug is an Associate Professor at the Vehicle Safety Institute, Graz University of Technology, Austria.

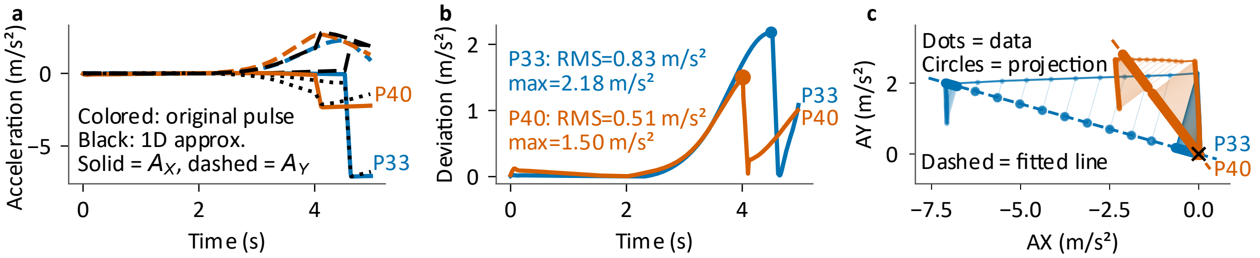

Fig. 1: Comparison of original and approximated acceleration pulses 33 and 40 from UTYP 141 GIDAS. (a) Measured acceleration components $\boldsymbol{a}_{\boldsymbol{x}}(t)$ and $\boldsymbol{a}_{\boldsymbol{y}}(t)$ and their one-dimensional approximations obtained by projection onto the principal direction, (b) deviation magnitude between the original and approximated pulses over time, including RMS and maximum error values quantifying the approximation accuracy and, (c) projection of $\boldsymbol{a}_{\boldsymbol{x}}(t)$ - $\boldsymbol{a}_{\boldsymbol{y}}(t)$ plane together with the fitted principal directions.

III. INITIAL FINDINGS

The optimised sled-pulse and seat-orientation combinations reproduce the targeted coupled longitudinal-lateral acceleration profiles with high fidelity, despite the intrinsic coupling of lateral and longitudinal sled motions (Fig. 1a, b). For pulse 33 the RMS error is 0.83 m s^{-2} (max 2.18 m s^{-2}) with a 16° seat rotation; pulse 40 yields a lower RMS error of 0.51 m s^{-2} (max 1.50 m s^{-2}) requiring a 53° rotation about the z-axis. Numerical integration of the projected accelerations provides the corresponding velocity and displacement histories, from which the required sled track lengths are estimated (pulse 33: 1.36 m; pulse 40: 3.16 m), see Fig. 2. The latter approaches the experimental sled's 2 × 1.875 m limit, necessitating precise initial seat positioning to fully exploit the available travel range (Fig. 2).

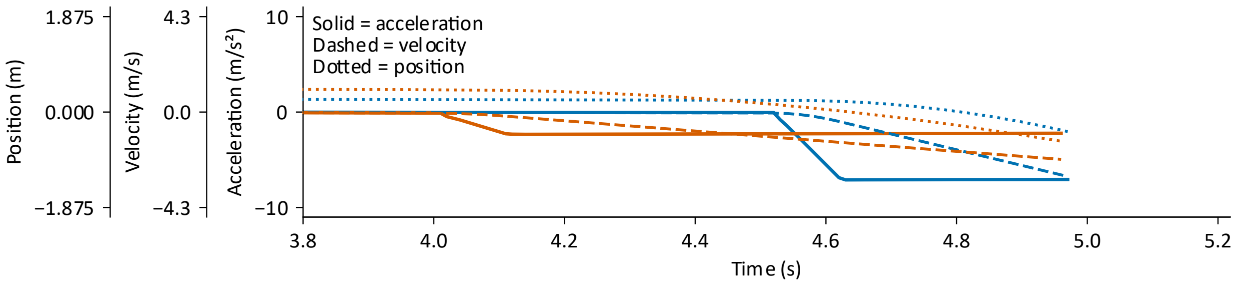

Fig. 2: Comparison of sled acceleration pulses 33 and 40 with respect to the operational limits of the sled system. The time histories of acceleration (solid), velocity (dashed), and displacement (dotted) are shown using separate y-axes on the left, each scaled in its physical unit. The axis ticks indicate the corresponding system limits for acceleration (±10 m/s²), velocity (±4.3 m/s), and displacement (±1.875 m), allowing a direct assessment of whether the generated pulses remain within the allowable operating range of the sled.

IV. DISCUSSION

Our first-order optimisation framework successfully generates realistic run-off-road acceleration pulses and the required seat orientations within the limits of a low-G sled, accurately reproducing the coupled longitudinal-lateral dynamics observed in CEDATU and GIDAS events of run-off-road accidents with subsequent collisions with objects or obstacles. Consequently, the method offers a robust, reproducible basis for designing and validating volunteer pre-crash studies on low-G test benches with rotated seats.

In a future step, human body model simulations could be used to assess how well the approximated pulses preserve the key kinematic features driving restraint-system engagement. Future work will systematically compare optimisation metrics based on occupant responses and confirm the predictions through experimental volunteer tests.

V. REFERENCES

[1] Bechler, F., Shaker Verlag, Aachen, 2024.
[2] Östh, J. *et al.* Traffic Inj. Prev, 2015.
[3] GIDAS UTYP 141, GIDAS Database, 2021.
[4] Fahse, N. *et al,* GAMM Mitteilungen, 2023.
[5] Gstrein, G. et.al. IRCOBI, IRC-25-92, 2025.

We employed the open-source OpenAI GPT model, hosted on the GWDG infrastructure, for automated spelling checks and linguistic polishing of the manuscript.